International Journal of Mathematical Analysis Vol. 19, 2025, no. 4, 177 - 192 HIKARI Ltd, www.m-hikari.com https://doi.org/10.12988/ijma.2025.912595

Bifurcation Analysis of a Metapopulation Model with Dispersal Risk and Linear Harvesting in Fragmented Habitats 1

Yongxin Cen, Jingli Xie and Qing Shu

College of Mathematics and Statistics, Jishou University Jishou, Hunan 416000, P.R. China

This article is distributed under the Creative Commons by-nc-nd Attribution License. Copyright © 2025 Hikari Ltd.

Abstract

In this paper, we study the dynamical properties of a discrete linear harvesting metapopulation with diffusion. By using Euler iteration algorithm to discretize the space, we obtain the two-dimensional discrete-time model with diffusion. We survey the existence conditions and stability of the fixed points, the analysis of transcritical, pitchfork, and flip bifurcations of nonhyperbolic fixed points provided by using the center manifold theorem. Numerical simulations and biological explanation analyzes are made to demonstrate the effective of the theoretical analyzes and to present the relations between these bifurcations.

Keywords Discrete metapopulation model with harvesting; Stability; Centre manifold theorem; Bifurcation

¹This work is supported by the General Project of Science Research Fund of Hunan Provincial Education Department (No: 24C0251) and the Scientific Research Fund of Jishou University (No: JDY2024071).

1 Introduction

Habitat fragmentation is one of the most damaging ecological processes of our time and a major reason for global biodiversity loss. As human activities like city expansion, farming, and deforestation increase, about 30% of the world's land ecosystems have been broken into separate patches [1]. This pushes species extinction rates higher than natural levels [2] and forces populations to move between isolated habitat fragments to survive. The way populations change in this patchy landscape can't be described by older models that treated them as single, uniform groups like the logistic equation. Because of this, the concept of metapopulations populations made up of smaller groups living in separate patches has become essential for understanding how species survive in fragmented landscapes [3]. Its core idea is that movement between patches keeps these smaller populations viable.

However, the classic metapopulation approach, best known from Levins' simple model [4], treats patches as either occupied or empty, focusing on a balance between colonization and local extinction. This simplification misses two crucial realities: (1) populations change continuously in size, like density-dependent growth limited by resources and harvesting; and (2) the movement process itself is spatial and explicit, like the loss of individuals leaving edge patches. These gaps limit the model's ability to deal with human pressures (like fishing, hunting).

To address these limitations, we developed a two-patch metapopulation model for isolated habitats. It builds on models of populations with boundaries and discrete movement over time and space [5]. Using Euler iteration, we derived a model with discrete-time movement including a harvesting term:

$$\mu_i^{t+1} = r\mu_i^t (1 - \frac{\mu_i^t}{K}) - h(\mu_i^t) + d\Delta^2 \mu_{i-1}^t, \tag{1.1}$$

Here, r is the intrinsic growth rate, K is the carrying capacity, $h(u_i)$ is density-dependent harvest (we consider $h(u_i) = \varepsilon u_i$ in this paper), d is the movement rate, t is time (0, 1, 2,...), and Δ^2 is the second-order difference operator $(\Delta^2 \mu_{i-1}^t = \mu_{i+1}^t - 2\mu_i^t + \mu_{i-1}^t$, i = 1, 2, ..., n) [6], which measures how populations spread between neighboring patches.

To focus on the smallest scale of patch interaction, we use fixed boundary conditions ($\mu_0^t = 0 = \mu_{n+1}^t$) to represent isolated habitats like islands or forest fragments. This assumes the area outside the boundaries is unsuitable, causing

permanent loss when individuals leave [7]. Simplifying the model to just two patches (letting $x_n = \mu_1^n$, $y_n = \mu_2^n$) gives us this system:

$$\begin{cases} x_{n+1} = rx_n(1 - \frac{x_n}{K}) - h(x_n) + d(-2x_n + y_n), \\ y_{n+1} = ry_n(1 - \frac{y_n}{K}) - h(y_n) + d(x_n - 2y_n). \end{cases}$$
(1.2)

Traditional coupled population models typically assume habitat patches are directly adjacent and migration occurs losslessly, often using net dispersal forms like $d(y_n - x_n)$ that ignore losses from edge patches [8]. However, real landscapes frequently feature patches separated by unsuitable matrix habitats. Our Model (1.2) explicitly quantifies this loss through the term $-2dx_n$: for the left-edge patch x_n , dispersal occurs both to the adjacent patch dx_n and as irreversible loss to the unsuitable matrix dx_n , totaling $2dx_n$ lost [9]. With only dy_n arriving from the right patch, the net movement becomes $dy_n - 2dx_n$. This formulation aligns with ecological evidence showing reduced survival at edges due to higher predation risk [10] and failed recolonization [7], while providing a mechanistic explanation for the 37 precent increased failure rate near edges reported by Ries et al. [11] and confirmed across classified groups [12].

Proportional harvesting $h(x) = \varepsilon x$ works together with the migration mechanism, serving as a model example of scientific population management. This model nicely integrates several core concepts in ecology: density-dependent growth, spatial heterogeneity, dispersal risk, and human-induced disturbance.

This paper is structured as follows. Section 2 establishes the existence of fixed points in Model (1.2). Section 3 classifies their topological types. Sections 4-6 analyze transcritical bifurcation, pitchfork bifurcation, and flip bifurcation (with corresponding biological interpretations), alongside stability analysis of the fixed points. Finally, we perform numerical simulations to validate our findings.

2 Exitence of Fixed Points

Put

$$E_0 = (0,0), E_1 = \left(\frac{K(r-d-\varepsilon-1)}{r}, \frac{K(r-d-\varepsilon-1)}{r}\right),$$

$$E_2 = \left(-\frac{K}{2r}(1+\varepsilon-r+2d), \frac{K}{4dr}(1+\varepsilon-r+2d)^2\right),$$

$$E_3 = \left(-\frac{K}{2r}(1+\varepsilon-r+2d+\sqrt{(1+\varepsilon-r)^2-4d^2}), \frac{K}{2dr}(1+\varepsilon-r+2d)(1+\varepsilon-r)\right).$$

Theorem 2.1. We consider the havesting function can be $h(x) = \varepsilon x$ in system (1.2). Thus the fixed points of system (1.2) can be classifies as follows:

- (I) If x = y, system (1.2) has a trival fixed point E_0 , and a unqique non-negative fixed point E_1 . Let $\varepsilon_0 = r d 1$, as ε varies from left ($\varepsilon < \varepsilon_0$) to right ($\varepsilon > \varepsilon_0$), E_1 coalesces with E_0 at the origin ($\varepsilon = \varepsilon_0$) and moves along y = x, from the fourth quadrant to the first quadrant.
- (II) Assuming $x \neq y$, system (1.2) has four nonnegative fixed points, if the following conditions holds:
 - (ii) if $1 + \varepsilon r \neq = 2d$ is satisfied, E_2 is obtained.
 - (iii) if $(1 + \varepsilon r)^2 > 4d^2$ is satisfied, E_3 is obtained.

3 Topological types of the fixed point

Next we consider the dynamics of system (1.2) in the qualitative properties of each fixed point. Combining with the existence conditions of the positive fixed point E_0, E_1, E_2 and the location of these corresponding eigenvalue multipliers relative to the unit circle in the complex plane, we obtain the topological classifications of the fixed points E_0, E_1, E_2 are given by Table 1,2, 3.

Condition on d	Condition on ε	Topological Property	Case Label
d > 0	$\varepsilon > r - d + 1$	Unstable node	E_{0-UNF}
d < 1	$r - d - 1 < \varepsilon < r - 3d + 1$	Saddle with flip	E_{0-SF1}
$d \ge 1$	$r - d - 1 < \varepsilon < r - d + 1$	Saddle with flip	E_{0-SF2}
$d \ge 1$	$r - 3d - 1 < \varepsilon < r - 3d + 1$	Saddle with flip	E_{0-SF3}
$d \neq 1$	$\varepsilon = r - d - 1$	Non-hyperbolic	E_{0-NH1}
$d \neq -1$	$\varepsilon = r - d + 1$	Non-hyperbolic	E_{0-NH2}
$d \neq -1$	$\varepsilon = r - 3d - 1$	Non-hyperbolic	E_{0-NH3}
$d \neq 1$	$\varepsilon = r - 3d + 1$	Non-hyperbolic	E_{0-NH4}

Condition on d	Condition on ε	Topological Property	Case Label
d > 0	$\varepsilon < r + d - 3 \text{ or } \varepsilon > r + d - 1$	Unstable node	$E_{1-\text{UNF}}$
d > 0	$\varepsilon_0 < \varepsilon < r + d - 3$	Saddle with flip	E_{1-SF1}
$d \neq 1$	$\varepsilon = r + d - 3$	Non-hyperbolic	$E_{1-\mathrm{NH1}}$
d > 0	$\varepsilon = r + d - 1$	Non-hyperbolic	$E_{1-\mathrm{NH2}}$

Table 2: Topological Types of the Fixed Point E_1

Table 3: Topological Types of the Fixed Point E_2

Condition on d	Condition on ε	Topological Property	Case Label
d > 0	$\varepsilon = r - 2d - 1$	Saddle with flip	E_{2-SF1}
$0 < d < \frac{2}{6 + \sqrt{37}}$	$\varepsilon = 2d + r - 1$	Saddle with flip	E_{2-SF2}
$d > \frac{2}{6 + \sqrt{37}}$	$\varepsilon = 2d + r - 1$	Unstable node	$E_{2-\mathrm{UNN}}$
$d = \frac{2}{6 + \sqrt{37}}$	$\varepsilon = 2d + r - 1$	Non-hyperbolic	$E_{2-\mathrm{NH1}}$

Remark 3.1 For the degenerate case of the E_3 point, refer to Theorem 6.1.

4 Bifurcation at Fixed Point E_0, E_1

This section presents the bifurcations occurring at E_0 and E_1 , along with their corresponding biological interpretations.

Remark 4.1. A transcritical bifurcation occurs at E_0 when the parameter $\varepsilon_1 = r - d - 1 - \varepsilon$ crosses zero, corresponding to the non-hyperbolic case E_{0-NH1} in Table 1. Assume $d \neq 1$, and let $U \subset \mathbb{R}^n$ (resp. $V \subset \mathbb{R}$) be a small neighborhood of E_0 . Then, in the neighborhood $U \times V$, the following statements hold:

1. When $\varepsilon_1 > 0$ (i.e., $\varepsilon < r - d - 1$, low fishing intensity), E_0 is unstable, and a unique stable fixed point $\widetilde{E}_0 \in U$ emerges (bifurcates from E_0).

- 2. When $\varepsilon_1 < 0$ (i.e., $\varepsilon > r d 1$, high fishing intensity), E_0 is locally asymptotically stable (population collapses to extinction if perturbed).
- 3. When $\varepsilon_1 = 0$ (i.e., $\varepsilon = r d 1$, critical fishing intensity), E_0 is right-semi-asymptotically stable: trajectories starting from the right neighborhood of E_0 (small positive populations) converge to E_0 , while those from the left (small negative populations, biologically irrelevant) diverge.
- Remark 4.2. The fixed point E_0 undergoes a supercritical flip bifurcation when the parameter $\varepsilon_2 = r - d + 1 - \varepsilon$ passes through 0, as identified in the nonhyperbolic condition E_{0-NH2} (see Table 1). From a biological perspective, Theorem 6.1 implies that under constant fishing intensity:
 - 1. When $r d + 1 > \varepsilon$ ($\varepsilon_2 > 0$), the metapopulation exhibits stable period-2 oscillations around the Maximum Sustainable Yield (MSY) level.
 - 2. When $r d + 1 < \varepsilon$ ($\varepsilon_2 < 0$), the metapopulation stabilizes at the MSY level E_0 over the long term.
- **Remark 4.3.** System (1.2) undergoes a pitchfork bifurcation at the fixed point E_0 when parameter $\varepsilon_3 = r 3d 1 \varepsilon$ passes through 0, as indicated in E_{0-NH3} (see Table 1). The pitchfork bifurcation enables metapopulation coexistence at the critical harvesting intensity $\varepsilon_3 = r 3d 1$. This represents an ecological transition from extinction to sustainable coexistence.
- **Remark 4.4.** System (1.2) undergoes a flip bifurcation at E_0 , E_1 when parameter $\varepsilon_4 = r 3d + 1 \varepsilon$ passes through $0, \varepsilon = r + d 3$, as indicated in E_{0-NH4} (see Table 1), E_{1-NH1} in Table 2).
- **Remark 4.5.** When $\varepsilon = r + d 1$, mapping system (1.2) undergoes a pitchfork bifurcation at fixed point E_1 , as identified in E_{1-NH2} (see Table 2).

5 Bifurcation at Fixed Point E_2

In this section, we will investigate the bifurcations of the above non-hyperbolic fixed points by using the central manifold theorem and the normal form E_{2-NH3} (see Table3).

5.1 Flip Bifurcation of E_2

Theorem 5.1. System(1.2) undergoes a flip bifurcation at fixed point E_2 when $d_0 = 0$ (see E_{2-NH3} in Table 3), with the following characteristics:

- 1. Supercritical case: When $\frac{2k}{r} > 79 + 13\sqrt{37}$ and $\Delta > 0$, a stable period-2 orbit bifurcates for $d_0 > 0$ and E_2 is unstable.
- 2. Subcritical case: When $\frac{2k}{r} < 79 + 13\sqrt{37}$ and $\Delta < 0$, an unstable period-2 orbit bifurcates for $d_0 < 0$ and E_2 is asymptotically stable.

The critical diffusion coefficient $d^* = \frac{2}{6 + \sqrt{37}}$ determines stability: For $d > d^*$, E_2 is unstable; For $d < d^*$, E_2 is asymptotically stable.

Proof. Let

$$\mu = x + \frac{k(1+\varepsilon - r + 2d)}{2r}, \quad v = y - \frac{k(1+\varepsilon - r + 2d)^2}{4dr}, \quad d_0 = d - \frac{2}{6+\sqrt{37}}.$$

The system transforms to:

$$\begin{pmatrix} \mu \\ d_0 \\ v \end{pmatrix} \mapsto \begin{pmatrix} 1 & 0 & \frac{2}{6+\sqrt{37}} \\ 0 & 1 & 0 \\ \frac{2}{6+\sqrt{37}} & 0 & 1 \end{pmatrix} \begin{pmatrix} \mu \\ d_0 \\ v \end{pmatrix} + \begin{pmatrix} vd_0 - \frac{r}{k}\mu^2 \\ 0 \\ \mu d_0 - \frac{r}{k}v^2 \end{pmatrix}. \tag{5.1}$$

Apply the linear transformation:

$$\mu = \zeta + \eta$$
, $d_0 = \delta$, $v = -(6 + \sqrt{37})\zeta + (\sqrt{37} - 6)\eta$

to diagonalize (5.1):

$$\begin{pmatrix} \zeta \\ \delta \\ \eta \end{pmatrix} \mapsto \begin{pmatrix} -1 & 0 & 0 \\ 0 & 1 & 0 \\ 0 & 0 & 147 - 24\sqrt{37} \end{pmatrix} \begin{pmatrix} \zeta \\ \delta \\ \eta \end{pmatrix} + \begin{pmatrix} g_1(\zeta, \delta, \eta) \\ 0 \\ g_2(\zeta, \delta, \eta) \end{pmatrix}, \tag{5.2}$$

where

$$g_1(\zeta, \delta, \eta) = -2\eta \delta - 2\zeta \delta + \frac{r}{k} (79 + 11\sqrt{37}) \zeta^2$$

$$+ \frac{r}{k} (79 + 13\sqrt{37}) \eta^2 + \frac{2r}{k} (\sqrt{37} - 7) \zeta \eta,$$

$$g_2(\zeta, \delta, \eta) = (2 - 24\sqrt{37}) \eta \delta - (146 + 24\sqrt{37}) \zeta \delta$$

$$- \frac{r}{k} (79 + 13\sqrt{37}) \zeta^2 - \frac{r}{k} (79 - 11\sqrt{37}) \eta^2$$

$$+ \frac{2r}{k} (\sqrt{37} + 7) \zeta \eta.$$

The center manifold is given by $\eta = h(\zeta, \delta) = a\zeta^2 + b\zeta\delta + \mathcal{O}(3)$ with:

$$a = \frac{r(79 + 13\sqrt{37})}{k(292\sqrt{37} - 1776)}, \quad b = \frac{146 + 24\sqrt{37}}{2\sqrt{37}(148 - 24\sqrt{37})}.$$

Restricting (5.2) to the center manifold yields:

$$f(\zeta,\delta) = -\zeta - \frac{r(79+13\sqrt{37})}{k(292\sqrt{37}-1776)} \zeta^2 \delta - \frac{146+24\sqrt{37}}{74(148-24\sqrt{37})} \zeta \delta^2$$
$$-\frac{1}{\sqrt{37}} \zeta \delta + \frac{r}{2\sqrt{37}k} (79+11\sqrt{37}) \zeta^2$$
$$+\frac{r}{\sqrt{37}k} (\sqrt{37}-7) \frac{79+13\sqrt{37}}{292\sqrt{37}-1776} \zeta^3$$
$$+\frac{r}{\sqrt{37}k} (\sqrt{37}-7) \frac{146+24\sqrt{37}}{74(148-24\sqrt{37})} \zeta^2 \delta + \mathcal{O}(4).$$

The second iterate $f^2(\zeta, \delta)$ has the expansion:

$$f^{2}(\zeta,\delta) = \zeta + \frac{146 + 24\sqrt{37}}{74(148 - 24\sqrt{37})}\zeta\delta^{2} + \frac{1}{\sqrt{37}}\left(1 - \frac{r}{2k}(79 + 13\sqrt{37})\right)\zeta\delta + \frac{r}{\sqrt{37}k}\left(\sqrt{37} - 7\right)\left(\frac{79 + 13\sqrt{37}}{292\sqrt{37} - 1776} + 1\right)\zeta^{3} + \mathcal{O}(4).$$

Evaluating derivatives at $(\zeta, \delta) = (0, 0)$:

$$f|_{(0,0)} = 0, \quad \frac{\partial f}{\partial \zeta}\Big|_{(0,0)} = -1, \quad \frac{\partial f^2}{\partial \delta}\Big|_{(0,0)} = 0,$$

$$\frac{\partial^2 f^2}{\partial \delta^2}\Big|_{(0,0)} = 0, \quad \frac{\partial^3 f^2}{\partial \zeta^3}\Big|_{(0,0)} = \frac{6r}{\sqrt{37}k} \left(\sqrt{37} - 7\right) \left(\frac{79 + 13\sqrt{37}}{292\sqrt{37} - 1776} + 1\right),$$

$$\frac{\partial^2 f^2}{\partial \zeta \partial \delta}\Big|_{(0,0)} = \frac{1}{\sqrt{37}} \left(1 - \frac{r}{2k}(79 + 13\sqrt{37})\right).$$

The nondegeneracy condition is:

$$\Delta = \left(-\frac{\partial^3 f^2}{\partial \zeta^3}, \frac{\partial^2 f^2}{\partial \zeta \partial \delta} \right) \Big|_{(0,0)}$$

$$= \frac{-6r}{k} (\sqrt{37} - 7) \frac{305\sqrt{37} - 1692}{(292\sqrt{37} - 1776)} \left(1 - \frac{r}{2k} (79 + 13\sqrt{37}) \right)^{-1}.$$

By bifurcation theory [14], $\Delta > 0$ when $\frac{2k}{r} > 79 + 13\sqrt{37}$ (supercritical flip), and $\Delta < 0$ when $\frac{2k}{r} < 79 + 13\sqrt{37}$ (subcritical flip). For $d_0 = 0$, compute the

Schwarzian derivative of $f(\zeta, 0)$:

$$s(f(0)) = \frac{f'''(0)}{f'(0)} - \frac{3}{2} \left(\frac{f''(0)}{f'(0)}\right)^{2}$$

$$= \frac{6r}{\sqrt{37}k} (7 - \sqrt{37}) \frac{79 + 13\sqrt{37}}{292\sqrt{37} - 1776} - \frac{3r^{2}}{2 \cdot 37k^{2}} (79 + 11\sqrt{37})^{2}.$$

By [15], E_3 is unstable if $\Delta < 0$ and asymptotically stable if $\Delta > 0$.

Remark 5.2. From a biological perspective, Theorem 5.1 implies that in the absence of harvesting, the metapopulation exhibits period-2 fluctuations around the maximum environmental carrying capacity when the diffusion coefficient exceeds the critical value $d > d^*$. Conversely, if the diffusion coefficient is below d^* , the metapopulation asymptotically approaches the maximum carrying capacity, indicating a stable equilibrium. This highlights the role of diffusion in regulating population dynamics: high diffusion leads to oscillatory behavior, while low diffusion promotes stability.

6 Bifurcation at Fixed Point E_3

This section investigates bifurcations at non-hyperbolic fixed points using central manifold theory and normal forms.

6.1 Flip Bifurcation of E_3

Define $\theta = 1 + \varepsilon - r$. The flip condition at E_3 implies that the solution curve of

$$(2 - 3\theta - 6d)\left(2 + \sqrt{\theta^2 - 4d^2}\right) = d^2 \tag{6.1}$$

exists in the domain $\theta > 0$, $0 < d < \frac{2-3\theta}{6}$. Denote the solution of the equation (6.1) by $\widetilde{d}(\theta)$. When $d = \widetilde{d}(\theta)$, a flip bifurcation occurs at E_3 .

Apply the coordinate transformation: $\mu = x + \frac{K(1+\varepsilon-r+2d)+K\sqrt{(1+\varepsilon-r)^2-4d^2}}{2r}$, $\nu = y - \frac{K(1+\varepsilon-r+2d)}{r}$, $\delta = d - \widetilde{d}(\theta)$. The system becomes:

$$\begin{pmatrix} \mu \\ \nu \end{pmatrix} \mapsto \begin{pmatrix} 1 + \sqrt{\theta^2 - 4\left(\delta + \widetilde{d}(\theta)\right)^2} & \delta + \widetilde{d}(\theta) \\ \delta + \widetilde{d}(\theta) & 1 - 3\theta - 6\left(\delta + \widetilde{d}(\theta)\right) \end{pmatrix} \begin{pmatrix} \mu \\ \nu \end{pmatrix} + \begin{pmatrix} -\frac{r}{K}\mu^2 \\ -\frac{r}{K}\nu^2 \end{pmatrix} + \mathcal{O}(3).$$

$$(6.2)$$

Under the invertible transformation P:

$$P = \begin{pmatrix} 1 & S_2 \\ -\frac{\delta + \tilde{d}(\theta)}{-1 + \delta} & S_2 \frac{-(\delta + \tilde{d}(\theta))}{-1 + \delta} + 1 \end{pmatrix}, \tag{6.3}$$

where

$$S_{1} = -\widetilde{d}(\theta) \left[1 - 3\theta - 6\left(\delta + \widetilde{d}(\theta)\right) \right] \frac{1}{\delta + \widetilde{d}(\theta)} + \frac{\left[1 - 3\theta - 6\left(\delta + \widetilde{d}(\theta)\right) \right] \left(\delta + \widetilde{d}(\theta)\right)}{2 - 3\theta - 6\left(\delta + \widetilde{d}(\theta)\right)} + \delta + \widetilde{d}(\theta) + 1 - 3\theta - 6\left(\delta + \widetilde{d}(\theta)\right),$$

$$S_{2} = -\frac{S_{1}}{\delta - 1} - \frac{\delta + \widetilde{d}(\theta)}{2 - 3\theta - 6\left(\delta + \widetilde{d}(\theta)\right)} + 1 - \frac{\widetilde{d}(\theta)}{\delta + \widetilde{d}(\theta)},$$

the system simplifies to the Taylor series form:

$$\begin{pmatrix} \xi \\ \eta \end{pmatrix} \mapsto \begin{pmatrix} -1 + \delta & 0 \\ 0 & 1 - 3\theta - 6\widetilde{d}(\theta) - \widetilde{d}(\theta)S_1 \end{pmatrix} \begin{pmatrix} \xi \\ \eta \end{pmatrix} + \begin{pmatrix} \widetilde{f}_1(\xi, \delta, \eta) \\ \widetilde{f}_2(\xi, \delta, \eta) \end{pmatrix} + \mathcal{O}(4).$$
(6.4)

The coefficients are defined as:

$$\vartheta = 5\widetilde{d}(\theta) + \frac{\widetilde{d}(\theta)}{2 - 3\theta - 6\widetilde{d}(\theta)},\tag{6.5}$$

$$\rho = \frac{1 - 3\theta - 6\widetilde{d}(\theta)}{\widetilde{d}(\theta)} - 5 - \frac{1 + \frac{6\widetilde{d}(\theta)}{2 - 3\theta - 6\widetilde{d}(\theta)}}{2 - 3\theta - 6\widetilde{d}(\theta)} + \frac{1}{\widetilde{d}(\theta)},\tag{6.6}$$

$$\sigma = \frac{3\theta + 6\widetilde{d}(\theta) - 1}{\widetilde{d}^2(\theta)} + 6\frac{3\theta - 2}{\left(2 - 3\theta - 6\widetilde{d}(\theta)\right)^3} - \frac{1}{\widetilde{d}^2(\theta)}.$$
 (6.7)

The nonlinear terms are:

$$f_1(\xi, \delta, \eta) = \xi^2 - 2\vartheta \eta + 2\rho \delta \eta + 2\sigma \delta^2 \eta + \vartheta^2 \eta^2 + 2\rho \sigma \delta \eta^2 - 2\vartheta \sigma \delta^2 \eta^2 + o(4),$$

$$f_2(\xi, \delta, \eta) = d^2 \xi^2 + 2d(1+d)\delta \xi^2 + (\vartheta^2 d^2 - 2\vartheta d + 2 + 2d)\eta^2$$
(6.8)

$$f_{2}(\xi, \delta, \eta) = d^{2}\xi^{2} + 2d(1+d)\delta\xi^{2} + (\vartheta^{2}d^{2} - 2\vartheta d + 2 + 2d)\eta^{2}$$

$$+ 2\left[\vartheta^{2}d(1+d) - \vartheta\rho d^{2} + \rho d - (1+d)\vartheta\right]\delta\eta^{2}$$

$$- 2d^{2}\vartheta\xi\eta + \left[2d^{2}\rho - 3d(1+d)\vartheta - 2(1+d)\right]\delta\xi\eta + o(4).$$
 (6.9)

The reduced mappings are:

$$\widetilde{f}_{1}(\xi, \delta, \eta) = -\frac{r}{K} \left[\xi^{2} - 2\vartheta \eta + 2\rho \delta \eta + 2\sigma \delta^{2} \eta + \vartheta^{2} \eta^{2} - 2\rho \beta \delta \eta^{2} - 2\beta \sigma \delta^{2} \eta^{2} \right.$$

$$\left. + (1+d)(\rho - \vartheta) \left(\xi^{2} \delta - 2\beta \delta \eta + 2\rho \delta^{2} \eta + \vartheta^{2} \delta \eta^{2} \right) + \cdots \right] + o(4),$$

$$(6.10)$$

$$\widetilde{f}_{2}(\xi, \delta, \eta) = -\frac{r}{K} \left[df_{1}(\xi, \delta, \eta) + (1+d) \left(\xi^{2} \delta - 2\vartheta \delta \eta + 2\rho \delta^{2} \eta + \vartheta^{2} \delta \eta^{2} \right) + 2(1+d)\vartheta \delta^{2} \eta + f_{2}(\xi, \delta, \eta) \right] + o(4).$$

$$(6.11)$$

The center manifold $\eta = h(\xi, \delta)$ satisfies:

$$\eta = h(\xi, \delta) = a_1 \xi^2 + a_2 \xi \delta + a_3 \delta^2 + \mathcal{O}(3), \tag{6.12}$$

with coefficients:

$$a_2 = \frac{2r}{K} \frac{9d}{2 - 3\theta - 6d + 5d^2},\tag{6.13}$$

$$a_3 = \frac{2r}{K} \frac{d\vartheta}{3\theta + 6d - 5d^2 - \frac{2r}{K}\vartheta},\tag{6.14}$$

$$a_1 = \frac{r}{K} \frac{\left[-d - d^2 + 2\vartheta + \vartheta d^2 + (1 - d\vartheta)a_2 \right]}{3\theta + 6d - 5d^2 - \frac{4r}{K}\vartheta d}.$$
 (6.15)

The reduced mapping on the center manifold is:

$$f_{\delta} \colon \xi \mapsto -\xi + \delta \xi + \widetilde{f}_{1}(\xi, \delta, h(\xi, \delta)).$$
 (6.16)

The flip bifurcation conditions are:

$$\frac{\partial^2 f_\delta}{\partial \xi \partial \delta} = 1,\tag{6.17}$$

$$\frac{1}{2} \left(\frac{\partial^2 f_{\delta}}{\partial \xi^2} \right)^2 + \frac{1}{3} \left(\frac{\partial^3 f_{\delta}}{\partial \xi^3} \right)^3 = \frac{1}{2} \left[\frac{2r}{K} (1 - d\vartheta)(1 - 2\vartheta) \right]^2 + \frac{1}{3} \left(12 \frac{r}{K} \vartheta d^2 \right)^3 \neq 0.$$

$$(6.18)$$

Theorem 6.1. If $\frac{1}{2} \left[\frac{2r}{K} (1 - d\vartheta)(1 - 2\vartheta) \right]^2 + \frac{1}{3} \left(12 \frac{r}{K} \vartheta d^2 \right)^3 \neq 0$, then for sufficiently small δ , the mapping (6.16) undergoes a flip bifurcation at E_3 . The bifurcation is supercritical (stable period-2 orbit) if the expression is positive, and subcritical (unstable period-2 orbit) if negative.

7 Numerical simulations

In this section, we will give bifurcation diagrams to illustrate the bifurcation phenomenons. The bifurcation parameters are considered as followed.

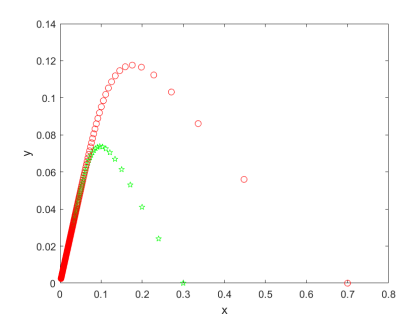


Fig. 1: transcritical bifurcation diagram in x - y plan in (0.3, 0), (0.7, 0)

Case 1: If set r = 2; $\varepsilon = 0.02$; d = 0.08; k = 5, we obtain system system (1.2) has a fixed point E_0 . The fixed point E_0 is a transcritical bifurcation point. From Fig. 1, when the initial value is (0.3,0), E_0 is unstable for $x \in (0,0.1)$, and becomes asymptotically stable at $y \in (0.06,0.08)$ when $x \in (0.1,0.3)$. Similarly, for the initial value (0.7,0), E_0 is unstable for $x \in (0,0.2)$, and begins to stabilize asymptotically at $y \in (0.1,0.12)$ when $x \in (0.2,0.7)$.

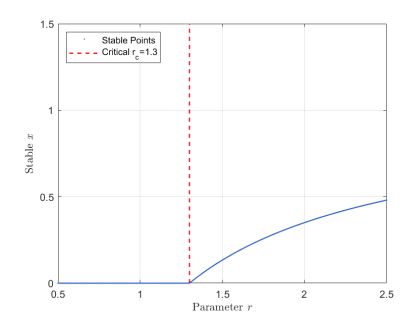


Fig. 2: pitchfork bifurcation in r - x plan in (0.1, 0.1)

Case 2: For system (1.2) with parameters $d = 0.2, K = 1, \varepsilon = 0.1$, bifurcation parameter $r \in (0.5, 2.5)$ and the initial value (0.1,0.1), the pitchfork bifurcation at E_1 unfolds as follows: when r < 1.3, x = 0 is the only stable equilibrium, so trajectories converge to x = 0; at r = 1.3, x = 0 loses stability; and for r > 1.3, x = 0, becomes unstable while two new stable equilibria

emerge, with the initial (0.1, 0.1) now converging to one of these new stable points.

Case 3: Consider system (1.2) with parameters $d=0.2, K=10, \varepsilon=0.1$, and bifurcation parameter $r\in(0,4)$, a supercritical flip bifurcation at $r\approx3.4$ occuers. Figure 2(a) displays the resulting dynamics in the r-x plane near E_1 with the initial conditions $(x_0,y_0)=(0.1,0.1)$, where increasing r beyond 3.4 initiates a cascade of period-doubling bifurcations leading to chaotic behavior.

The Maximum Lyapunov Exponents (MLE) in Fig.3(b) quantitatively confirm the bifurcation dynamics observed in Fig.3(a). At $r \approx 3.4$, the MLE transition from negative to positive values signifies the onset of chaos near equilibrium E₁, consistent with the supercritical flip bifurcation. Throughout the chaotic regime ($r \in [3.4, 3.5]$), the negative MLE values correspond to periodic windows embedded within the chaotic attractor. As r increases beyond 3.5, the systematic return to negative MLE values demonstrates stability restoration via inverse period-doubling bifurcations.

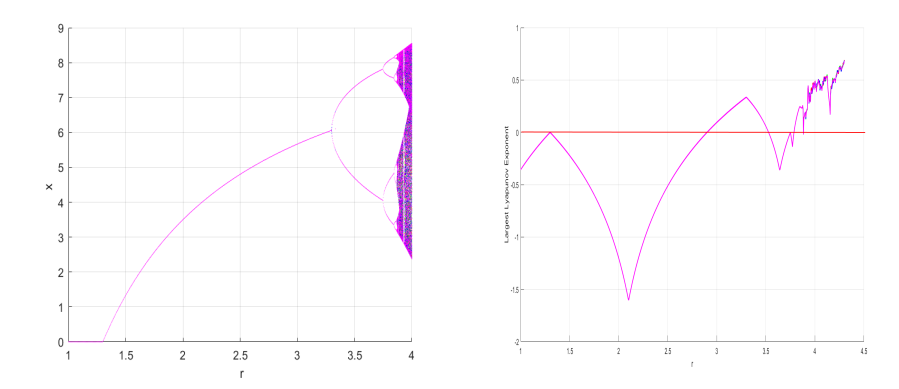


Fig. 3: (a) flip bifurcaton diagram in x-r plan in (0.1, 0.1),(b) Maximum Lyapunov exponents corresponding to (a)

Case 4: Let d = 0.012, $\varepsilon = 0.1$, k = 0.4574, and $r \approx 0.01091$; then $\theta = 0.6426$, which satisfies the condition $(2 - 3\theta - 6d)(2 + \sqrt{\theta^2 - 4d^2}) = d^2$. The superitical flip bifurcation originates from E_3 . Fig.4 depicts the two-dimensional superitical flip bifurcation diagram in the d - x plane near the fixed point E_3 as d ranges from 0.01 to 0.1.

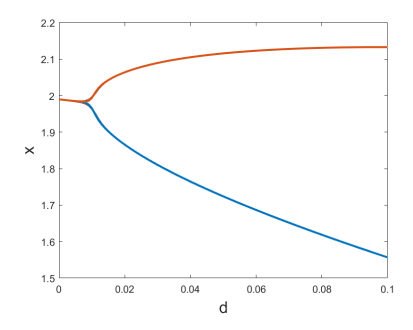


Fig. 4: Flip bifurcation diagram in the x-d plane when $d=0.012, \, \varepsilon=0.1, \, k=0.4574, \, {\rm and} \, \, r\approx 0.01091$

Conclusion

This paper analyzes the dynamics of a discrete-time diffusion model with linear harvesting. Through spatial discretization, a two-dimensional map is derived. The study focuses on the bifurcations near nonhyperbolic fixed points. For boundary points E_0 and E_1 , the existence of transcritical, pitchfork, and flip bifurcations is established and verified numerically (Figs. 1-3). Furthermore, a flip bifurcation is proven to occur at interior points E_3 and E_5 via center manifold theory, with complex dynamics like chaos also observed (Fig. 4).

The analysis provides biological insights: the metapopulation stabilizes at its maximum sustainable yield (Figs. 2, 3), or by restricting the harvesting rate below a critical value (Fig. 1). Stability is also achievable without harvesting by controlling the diffusion coefficient (Theorems 5.1, 6.1), underscoring its key role in maintaining stability under a constrained harvest.

References

- [1] Haddad, N. M. et al., Habitat fragmentation and its lasting impact on Earth's ecosystems, *Science Advances*, **1** (2) (2015), e1500052. https://doi.org/10.1126/sciadv.1500052
- [2] Ceballos, G. et al., Accelerated modern human-induced species losses: Entering the sixth mass extinction, *Science Advances*, **1** (5) (2015), e1400253. https://doi.org/10.1126/sciadv.1400253

- [3] Hanski, I., *Metapopulation ecology*, Oxford University Press, 1999. https://doi.org/10.1093/oso/9780198540663.001.0001
- [4] Levins, R., Some demographic and genetic consequences of environmental heterogeneity for biological control, Bulletin of the Entomological Society of America, 15 (3) (1969), 237–240. https://doi.org/10.1093/besa/15.3.237
- [5] Hastings, A. & Higgins, K., Persistence of transients in spatially structured ecological models, *Science*, 293 (5530) (2001), 627–630.
 https://doi.org/10.1126/science.263.5150.1133
- [6] Turchin, P., Quantitative analysis of movement, Sinauer Associates, 1998.
- [7] McDonald, D. B. & Caswell, H., The demographic and habitat requirements of northern spotted owls, *Ecological Modelling*, **62** (1992) (1–3), 151–162.
- [8] Allen, J. C. et al., Chaos reduces species extinction by amplifying local population noise, *Nature*, 364 (1993), 229–232.
 https://doi.org/10.1038/364229a0
- [9] Gonzalez, A. et al., Scaling-up biodiversity-ecosystem functioning research, *Landscape Ecology*, 38 (8) (2023), 1867–1880.
- [10] Fahrig, L., Effects of habitat fragmentation on biodiversity, Annual Review of Ecology, Evolution, and Systematics, 34 (2003), 487–515. https://doi.org/10.1146/annurev.ecolsys.34.011802.132419
- [11] Ries, L. et al., Ecological responses to habitat edges, Annual Review of Ecology, Evolution, and Systematics, 35 (2004), 491–522. https://doi.org/10.1146/annurev.ecolsys.35.112202.130148
- [12] Bergerot, B. et al., Prioritizing green infrastructure locations to reduce fragmentation, Global Ecology and Biogeography, 30 (5) (2021), 1033–1046.
- [13] Kuznetsov Y.A., Elements of Applied Bifurcation Theory, 3rd ed., Springer, New York, 2004. https://doi.org/10.1007/978-1-4757-3978-7

- [14] Guckenheimer J., Holmes P., Nonlinear Oscillations, Dynamical Systems, and Bifurcations of Vector Fields, Springer, New York, 1983. https://doi.org/10.1007/978-1-4612-1140-2
- [15] Dannan F., Elaydi S., Ponomarenko V., Stability of hyperbolic and non-hyperbolic fixed points of one-dimensional maps, *Journal of Difference Equations and Applications*, 9 (5) (2003), 449–457. https://doi.org/10.1080/1023619031000078315

Received: September 30, 2025; Published: October 11, 2025